Hyperspectral Endmember Material Identification Using Spectral Library Matching

Nian Zhang, Fred Rischmiller, and Wagdy H. Mahmoud

University of the District of Columbia
Department of Electrical and Computer Engineering
Washington, D.C., 20008, USA
nzhang@udc.edu, frederick.rischmille@udc.edu, and wmahmoud@udc.edu

Abstract. Hyperspectral imaging provides a powerful means of material identification by capturing detailed spectral information across a broad range of wavelengths. However, the accurate classification of materials remains challenging due to spectral mixing and the lack of ground truth data. This paper proposes a robust approach for hyperspectral endmember extraction and material identification by integrating the N-FINDR algorithm with spectral information divergence (SID)-based spectral library matching. The proposed method enhances segmentation accuracy by identifying pure spectral signatures (endmembers) and associating them with actual materials using the ECOSTRESS spectral library. Experimental validation using the Pavia University hyperspectral dataset demonstrates the effectiveness of this approach in extracting, identifying, and segmenting endmember materials with high precision. The results underscore the advantages of combining geometric-based endmember extraction with spectral matching techniques to improve hyperspectral image analysis.

Keywords: Endmember extraction, spectral unmixing, N-FINDR, spectral information divergence (SID), spectral library matching, spectral classification, hyperspectral image segmentation.

1 Introduction

Hyperspectral imaging captures a broad spectrum of wavelengths, with each spectral band corresponding to a specific wavelength of light [1]-[10]. This technique enables the identification of materials or objects based on their spectral signatures—distinctive patterns of reflectance or emittance across different wavelengths. Unlike conventional imaging, hyperspectral imaging captures both spatial and spectral data [11]. It not only includes visible spectrum, but also includes ultraviolet (UV) and long-wave infrared (LWIR) wavelengths. Because it covers the visible, near-infrared, and mid-infrared regions, hyperspectral images can capture highly detailed spectral information with narrow, adjacent wavelength bands within a defined spectral range [12]. This capability is particularly valuable in remote sensing, where it helps distinguish features such as vegetation, water bodies, and infrastructure based on their unique spectral characteristics [13]. Its ability to provide intricate spectral information makes hyperspectral imaging essential for applications like target detection, material identification, and surface classification.

The main objective of hyperspectral image analysis is to enhance classification and mapping accuracy. However, two major obstacles impede this goal [14]. The first is the lack of sufficient ground truth labels or limited training samples, which results in the Hughes effect. This effect causes classification performance to decrease because when the number of spectral features increases, the classification tends to be less accurate. The second challenge is spectral mixing, which is caused by the sensor's spatial resolution or when multiple surface materials are contained within a single pixel. As a result, the spectral reflectance of different materials blends in a linear fashion, complicating the accurate categorization of mixed pixels into distinct material classes.

To address these challenges, endmembers extraction has emerged as a powerful solution to mitigate the effects of the Hughes effect and spectral mixing, which can result in enhanced classification performance [15]. Endmembers are the purest pixel spectra in the hyperspectral image, which ideally represent a unique material or substance in the scene. Endmember extraction (EE) is a crucial process that involves identifying the pure spectral signatures that represent the different materials present in a remotely sensed hyperspectral image.

Existing endmember extraction or identification algorithms are designed to extract the most pure, representative spectra (endmembers) from hyperspectral images. These algorithms play a crucial role in hyperspectral image analysis by identifying distinct spectral signatures that represent the materials or objects present in the scene. However, despite their importance, a common limitation across all these methods is that they focus on extracting the spectral features and do not automatically link the extracted endmembers to real-world materials or classes.

To address the limitation of material identification, several approaches have been developed. One such approach is *Spectral Library Matching*. This method links the extracted endmembers to specific materials by comparing them with spectral libraries containing known material spectra. When an extracted endmember closely matches a reference spectrum in the library, the material corresponding to that spectrum can be identified. This technique relies heavily on the availability of comprehensive spectral libraries and is a straightforward way to label endmembers based on known material signatures.

To interpret the extracted endmembers effectively, we will propose a hyperspectral endmember extraction and material identification method by combining the N-FINDR algorithm with spectral information divergence-driven spectral library matching.

The remainder of the paper is organized as follows. Section II provides the literature review. Section III provides the details of the proposed method, including the N-FINDR endmember extraction algorithm and the spectral information divergence (SID) spectral matching method. Section IV described the Pavia University hyperspectral image dataset. It also demonstrates experimental results. Section V provides the conclusions.

2 Literature Review

Endmember extraction is a vital task in hyperspectral image analysis, focused on identifying the purest spectral signatures (endmembers) that represent the materials or objects in the scene. Various methods have been developed for endmember extraction, which have their unique advantages and limitations. These methods can be generally grouped into the following categories.

1) *Geometric Approaches*: One of the most widely used methods for endmember extraction is the vertex component analysis (VCA) [16]. VCA exploits the geometry of the data by looking for the vertices of the convex hull formed by the spectra in high-dimensional space. This method is efficient and can handle large datasets. However, the main limitation of VCA is its assumption of spectral purity, which can lead to issues when spectral mixing occurs in complex scenes. The N-FINDR algorithm [17] (N-dimensional Iterative Spectral Mixture Analysis) is another geometric approach that identifies endmembers by maximizing the volume of the simplex formed by a set of selected pixels in the spectral space. The algorithm iteratively selects pixels that best represent the purest endmembers, and its output is the set of endmembers that corresponds to the highest volume simplex. While N-FINDR is known for its simplicity and effectiveness in extracting endmembers from relatively simple datasets, it can struggle when spectral mixing is prevalent or when there is a high degree of noise in the data.

2) *Statistical Approaches*: In contrast to geometric methods, statistical approaches to endmember extraction focus on the statistical properties of the hyperspectral data. One prominent example is independent component analysis (ICA) [18], which aims to extract statistically independent components from hyperspectral data. Unlike Principal Component Analysis (PCA), which seeks orthogonal components, ICA identifies components that are statistically independent. ICA is particularly useful when the data involve mixed signals, and it has been successfully applied to remote sensing tasks where endmembers correspond to independent materials in a scene. However, the assumption of statistical independence may not always hold in real-world scenarios, especially when the endmembers are spectrally similar. Another popular statistical technique is Principal Component Analysis (PCA) [19]. PCA reduces the dimensionality of hyperspectral data by transforming the original spectra into a set of orthogonal components. PCA can be used for endmember extraction by selecting the components that best represent the spectral variation in the data. However, PCA often struggles to directly identify physical endmembers, as it tends to mix spectral information from different materials in the same component.

3) *Optimization-Based Approaches*: Optimization-based techniques focus on finding the set of endmembers that most accurately represent the hyperspectral data by minimizing a defined objective function. A common method is Spectral Mixture Analysis (SMA) [20], which posits that each pixel in the image is a combination of multiple endmembers. The objective of SMA is to identify the endmembers that, when combined, provide the closest match to the observed pixel spectra. SMA has the advantage of being able to model mixed pixels, making it particularly useful in heterogeneous environments. However, it requires accurate initial estimates of endmembers and can be computationally intensive. Another optimization-based approach is the Sparse Unmixing technique [21], which aims to decompose hyperspectral data into a sparse combination of endmembers. This method exploits the assumption that only a few endmembers are present in each pixel, and it uses optimization algorithms to find a sparse representation of the data. Sparse unmixing has gained popularity in recent years due to its ability to handle mixed pixels and its ability to extract endmembers even when the data is highly corrupted by noise. However, one of the challenges with sparse unmixing is that it requires careful tuning of regularization parameters to ensure optimal performance.

4) *Hybrid Approaches*: Recently, there has been an increasing interest in hybrid methods that combine multiple endmember extraction techniques. For example, semi-supervised learning techniques [22] have been employed to improve endmember extraction by integrating endmember identification with machine learning classifiers. These hybrid approaches use labeled data to refine the extraction process and can significantly improve accuracy in complex scenes where traditional methods may struggle. Notably, promising hybrid approach involves combining spectral library matching with endmember extraction [23]. In this method, the endmembers extracted using traditional techniques are matched to a spectral library of known materials. By comparing the extracted endmembers to reference spectra, researchers can identify the materials represented by the endmembers. This approach has the advantage of automating the identification process, though it still relies on the availability of a comprehensive and accurate spectral library.

3 Proposed Methodology

3.1 Endmember Extraction

N-FINDR (N-dimensional-FINDing Endmembers Algorithm) is an algorithm designed to automatically find endmembers in hyperspectral images, which are the pure spectral signatures of materials in a given hyperspectral dataset. The algorithm assumes that each pixel in the hyperspectral image is a mixture of several endmembers, and it identifies a set of endmembers within the dataset. Below is the proposed N-FINDR algorithm.

Input:

- $X \in \mathbb{R}^{m \times n}$: Hyperspectral data matrix (with m bands and n pixels)
- K: The number of endmembers to be found.
- T_{max}: The maximum number of iterations for the algorithm.

Initialization:

- Select an initial random subset of K pixels from the dataset as candidate endmembers. This subset can be chosen randomly or based on some heuristics.

Compute the Spectral Geometry:

- For each combination of the selected endmembers, the algorithm computes a measure of how well the selected endmembers span the data. The measure typically used is the volume of the simplex formed by the candidate endmembers, which is used to evaluate the diversity and spread of the endmembers in the high-dimensional space.

Iterative Process:

- For each iteration:
    1. Compute the Spectral Volume:
        - For the current selection of endmembers, calculate the volume of the simplex they form. The volume is a measure of the spread of the endmembers in the hyperspectral space.
        - The volume V of the simplex formed by endmembers is given by the determinant of a matrix formed by the endmember vectors.

2. Select the next candidate:
    - The next step involves selecting a pixel from the dataset that will increase the volume of the simplex. This can be done by replacing one of the current endmembers with a pixel that increases the volume.
3. Evaluate and update the selection:
    - If the new selection improves the spectral volume (i.e., it increases the diversity of the endmembers), update the endmembers. Otherwise, keep the existing ones.

Stopping Criteria:

- The algorithm stops when the maximum number of iterations T_{max} is reached or when no improvement in volume is observed (i.e., the endmembers are stable).

Output:

- The final set of K endmembers that best represent the data.

3.2 Spectral Information Divergence (SID)

Spectral matching is a critical process in analyzing pixel spectra, because it can link an endmember to a material class [24]. This process involves comparing the endmember's spectrum with reference spectra from spectral libraries and measuring the differences in spectral information. In this paper, the ECOSTRESS spectral library is utilized as the reference, which is a comprehensive collection of spectral signatures for various natural and artificial materials. After loading the reference spectra from the ECOSTRESS library, we evaluate their similarity to the endmember spectrum by examining both the geometric characteristics and the probability distribution of the pixel spectra. This integrated information can improve the ability to differentiate spectrally similar targets within the same class. Spectral similarity is measured using the spectral information divergence (SID) method, which quantifies the divergence between the probability distributions of pixel spectra in a hyperspectral dataset and reference spectra. The proposed spectral information divergence (SID) algorithm is described below.

Given two spectra, S_1 and S_2, we normalize them and ensure that their sum equals 1. This helps convert the spectra into probability distributions.

$$S_1{}^{norm} = \frac{S_1}{\sum_{i=1}^{n} S_1(i)} \text{ and } S_2{}^{norm} = \frac{S_2}{\sum_{i=1}^{n} S_2(i)} \quad (1)$$

Where *n* is the number of spectral bands.

SID is calculated using the Kullback-Leibler (KL) divergence between the two normalized spectra. The formula for SID between two spectra $S_1{}^{norm}$ and $S_2{}^{norm}$ is given by:

$$SID(S_1, S_2) = D_{KL}(S_1{}^{norm} || S_2{}^{norm}) + D_{KL}(S_2{}^{norm} || S_1{}^{norm}) \quad (2)$$

where $D_{KL}(P||Q)$ represents the Kullback-Leibler divergence, which is defined as:

$$D_{KL}(P||Q) = \sum_{i=1}^{n} P(i) \log\left(\frac{P(i)}{Q(i)}\right) \quad (3)$$

where P(i) represents the normalized value of spectrum $S_1{}^{norm}$,

Q(i) represents the normalized value of spectrum $S_2{}^{norm}$.

The Kullback-Leibler (KL) divergence measures how one distribution (the actual spectrum) diverges from the expected distribution (the reference spectrum).

4 Experimental Results

4.1 Pavia University Dataset

The Pavia University dataset is a widely used hyperspectral image dataset captured by the Reflective Optics System Imaging Spectrometer (ROSIS-03) sensor over the University of Pavia, Italy. It consists of 610 × 340 pixels with 103 spectral bands covering the 0.43-0.86 μm wavelength range [25]. The dataset includes ground truth labels for nine land cover classes, such as asphalt, meadows, and trees, making it a benchmark for hyperspectral image classification tasks, as shown in TABLE I.

TABLE I. THE PAVIA UNIVERSITY CLASSES AND THEIR RESPECTIVE GROUND TRUTH SAMPLE NUMBER

#	**Class**	**Samples**
1	Asphalt	1,890
2	Meadows	2,830
3	Gravel	2,210
4	Trees	1,350
5	Painted Metal Sheets	520
6	Bare Soil	720
7	Bitumen	210
8	Bricks	1,020
9	Cement	2,430

4.2 Endmember Spectra Extraction

The following analysis will use the spectral signatures from the ECOSTRESS spectral library [26] as reference spectra and a sample from the Pavia University dataset as test data for identifying endmember materials.

We read the spectral information corresponding to different material from the ECOSTRESS spectral library by using the *readEcostressSig* function. The materials include roof material, concrete, road, mollisol, utisol, tree, ice, tap water, and sea water. The reference spectra from the ECOSTRESS library are shown in Fig. 1.

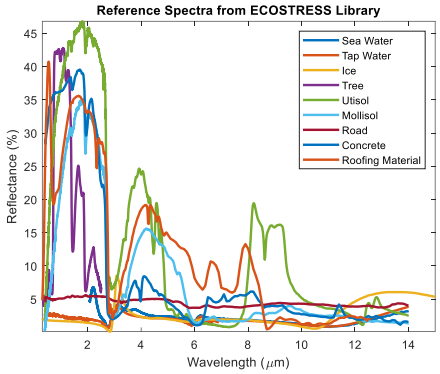

Fig. 1. Spectral signatures read from the ECOSTRESS spectral library.

We load the test data from the Pavia University dataset using the *hypercube* function, which produces a hypercube object containing both the data cube and its corresponding metadata. The test data contains 9 endmembers latent that includes Asphalt, Meadows, Gravel, Trees, Painted Metal Sheets, Bare Soil, Bitumen, Bricks, Cement.

To determine the total number of spectrally distinct endmembers in the test data, we use the *countEndmembersHFC* function. This function estimates the number of endmembers based on the *Harsanyi-Farrand-Chang (HFC)* method. To minimize false detections, we set the probability of false alarm (PFA) to a low value (i.e. 10^{-27}).

We then extract the endmembers from the test data using the N-FINDR method. We retrieve the wavelength values from the hypercube object and then plot the extracted endmember signatures, as shown in Fig. 2.

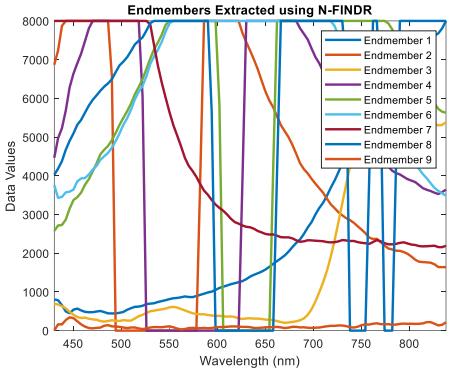

Fig. 2. Full spectra of the extracted endmember signatures using the N-FINDR method.

4.3 Endmember Material Identification Using Spectral Library

In this experiment, we calculate the similarity between a reference spectrum from the library and a test spectrum to be classified using the spectral information divergence (SID) method.

The SID function computes the matching score between two spectra based on their probability distributions. Generally, a lower SID score indicates a better match between the test and reference spectra. The test spectrum is then classified as belonging to the class of the reference spectrum that provides the best match.

To classify the second and fourth endmember materials, we assess the spectral similarity between the reference spectra from the library and the corresponding endmember spectra. The class corresponding to the index with the lowest SID score is assigned to each endmember. Consequently, the second endmember is identified as Soil, and the fourth endmember is identified as Tree.

4.4 Segment Endmember Regions in Test Data

To visually inspect the identification results, we localize and segment the image regions corresponding to the endmember materials in the test data. We use the *sid* function to calculate the pixel-wise spectral similarity between the pixel spectrum and the extracted endmember spectrum. Next, we apply thresholding to segment the target endmember regions in the test data and generate the segmented image. We set the threshold value to 15 to identify the best matching pixels.

To enhance visualization and interpretation, we generate an RGB image of the test data using the *colorize* function.

Then we create an overlay of the segmented Soil (endmember 2) and Tree (endmember 4) endmember regions on the RGB image.

We display the binary segmentation results for the Soil (endmember 2) and Tree (endmember 4) endmember regions, as shown in Fig. 3. Fig. 3 (a) exhibits the binary segmentation results of the Soil (endmember 2) endmember region, and Fig. 3 (b) shows the binary segmentation results of the Tree (endmember 4) endmember region.

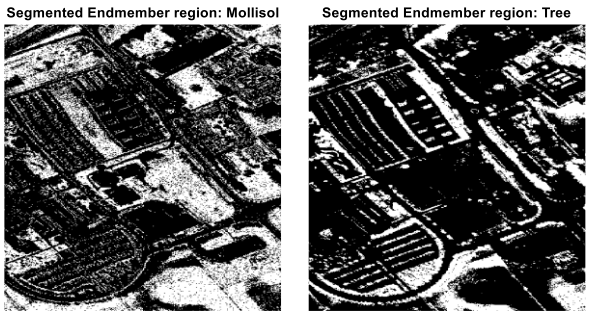

(a) (b)

Fig. 3. Segmented images of endmember 2 (Soil) and endmember 4 (Tree). (a) The binary segmentation results of the endmember 2 (Soil) endmember region. (b) The binary segmentation results of the endmember 4 (Tree) endmember region.

In addition, an RGB version of the test data is created, and an overlay of the segmented Soil and Tree endmember regions are added to the RGB image as shown in Fig. 4. Fig. 4 (a) is the RGB transformation of the test data, and Fig. 4 (b) displays an overlay of the segmented endmember 2 (Soil) and endmember 4 (Tree) endmember regions on the RGB image.

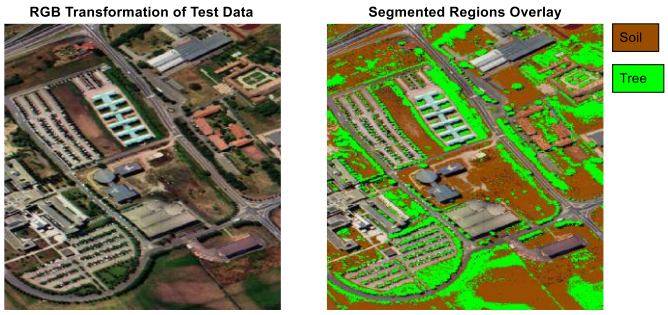

(a) (b)

Fig. 4. (a) RGB transformation of the test data. (b) An overlay of the segmented endmember 2 (Soil) and endmember 4 (Tree) endmember regions on the RGB image.

5 Conclusions

This paper proposes a framework for endmember extraction and material identification in hyperspectral image analysis. The approach develops an N-FINDR algorithm for spectral endmember extraction. In addition, it designs a spectral information divergence (SID) method to identify those materials by matching the extracted endmembers with reference spectra from the ECOSTRESS spectral library. The experimental results highlighted the effectiveness of the proposed method in accurately identifying materials within hyperspectral images. The segmentation results further validated the capability of the proposed approach in localizing specific materials in hyperspectral data. The findings underscore the importance of combining spectral matching techniques with endmember extraction for improved classification and material identification in hyperspectral imaging applications.

6 Future Work

Future research could focus on enhancing the coverage and diversity of spectral libraries, such as ECOSTRESS, to improve material classification accuracy. In addition, integrating deep learning techniques, including convolutional neural networks (CNNs) and transformer-based models, could further automate and refine endmember identification by learning complex spectral patterns. Additionally, addressing spectral variability caused by environmental factors like lighting conditions, atmospheric effects, and sensor noise would enhance the robustness of classification methods. Optimizing the N-FINDR and spectral information divergence (SID) algorithms for

real-time processing would also be beneficial, enabling faster hyperspectral image analysis in practical applications. Finally, exploring hybrid approaches that combine traditional spectral matching with statistical and machine learning methods could lead to more robust and adaptable hyperspectral imaging solutions.

Acknowledgment

This work is supported by the National Science Foundation (NSF) grants #2011927 and #2401880.

References

1. Rochac, J.F.R., Zhang, N., Thompson, L., Deksissa, T.: A robust context-based deep learning approach for highly-imbalanced hyperspectral classification. *Comput. Intell. Neurosci.* 9923491 (2021). https://doi.org/10.1155/2021/9923491
2. Zhang, N., Rouamba, S., Mahmoud, W., Thompson, L.: Hyperspectral image analysis using maximum abundance classification. In: *Proc. 13th Int. Conf. Intelligent Control and Information Processing (ICICIP 2025)*, Muscat, Oman, 6–11 Feb 2025
3. Baker-Adell, K., Zhang, N., Denis, M.: Semantic neuroanatomical segmentation of brain MRI scans using pretrained SynthSeg neural network. In: *Proc. 13th Int. Conf. Intelligent Control and Information Processing (ICICIP 2025)*, Muscat, Oman, 6–11 Feb 2025
4. Zhang, N., Thompson, L.: Classifying land cover using hyperspectral image and LiDAR data. In: *Proc. 13th Int. Conf. Intelligent Control and Information Processing (ICICIP 2025)*, Muscat, Oman, 6–11 Feb 2025
5. Zhang, N., Mahmoud, W.: Target detection in hyperspectral imagery using spectral signature matching algorithms. In: *Proc. 13th Int. Conf. Intelligent Control and Information Processing (ICICIP 2025)*, Muscat, Oman, 6–11 Feb 2025
6. Zhang, N., Wilson, O., Thompson, L.: Target identification and detection using hyperspectral signature transformation. In: *Proc. 13th Int. Conf. Intelligent Control and Information Processing (ICICIP 2025)*, Muscat, Oman, 6–11 Feb 2025
7. Rouamba, S., Zhang, N., Mahmoud, W.H., Thompson, L., Denis, M., Deksissa, T.: Hyperspectral image classification using custom spectral convolutional neural networks (CSCNNs). In: *Proc. 14th Int. Conf. Information Science and Technology (ICIST 2024)*, Chengdu, China, 6–9 Dec 2024
8. Rochac, J.F.R., Thompson, L., Zhang, N., Oladunni, T.: A data augmentation-assisted deep learning model for high dimensional and highly imbalanced hyperspectral imaging data. In: *Proc. 9th Int. Conf. Information Science and Technology (ICIST 2019)*, Hulunbuir, China, 2–5 Aug 2019
9. Rochac, J.F.R., Zhang, N., Behera, P.: Design of adaptive feature extraction algorithm based on fuzzy classifier in hyperspectral imagery classification for big data analysis. In: *Proc. 12th World Congress on Intelligent Control and Automation (WCICA 2016)*, Guilin, China, pp. 1046–1051 (2016)
10. Rochac, J.F.R., Zhang, N.: Feature extraction in hyperspectral imaging using adaptive feature selection approach. In: *Proc. 8th Int. Conf. Advanced Computational Intelligence (ICACI 2016)*, Chiang Mai, Thailand, pp. 36–40 (2016)
11. Chang, C.I., Kuo, Y.M., Hu, P.F.: Unsupervised rate distortion function-based band subset selection for hyperspectral image classification. *IEEE Trans. Geosci. Remote Sens.* 61, 1–18 (2023). https://doi.org/10.1109/TGRS.2023.3296728

12. Ertürk, A., Erten, E.: Unmixing of pollution-associated sea snot in the near surface after its outbreak in the Sea of Marmara using hyperspectral PRISMA data. *IEEE Geosci. Remote Sens. Lett.* 20, 1–5 (2023). https://doi.org/10.1109/LGRS.2023.3238962
13. Özdemir, O.B., Koz, A.: 3D-CNN and autoencoder-based gas detection in hyperspectral images. *IEEE J. Sel. Top. Appl. Earth Obs. Remote Sens.* 16, 1474–1482 (2023). https://doi.org/10.1109/JSTARS.2023.3235781
14. He, X., Chen, Y., Huang, L.: Toward a trustworthy classifier with deep CNN: uncertainty estimation meets hyperspectral image. *IEEE Trans. Geosci. Remote Sens.* 60, 1–15 (2022). https://doi.org/10.1109/TGRS.2022.3176913
15. Zhang, N., Mahmoud, W.H.: Convex geometry based endmember extraction for hyperspectral images classification. In: *Proc. 13th Int. Conf. Information Science and Technology (ICIST 2023)*, Cairo, Egypt, 8–14 Dec 2023
16. Chang, C.I., Bekit, A.: Endmember finding in compressively sensed band domain. In: Chang, C.I. (ed.) *Advances in Hyperspectral Image Processing Techniques*. Wiley. https://doi.org/10.1002/9781119687788.ch8
17. Chang, C.-I., Kuo, Y.-M., Hu, P.F.: Unsupervised rate distortion function-based band subset selection for hyperspectral image classification. *IEEE Trans. Geosci. Remote Sens.* 61, 1–18 (2023). https://doi.org/10.1109/TGRS.2023.3296728
18. Zhang, T., et al.: Multibaseline interferometry based on independent component analysis and InSAR combinatorial modeling for high-precision DEM reconstruction. *IEEE Trans. Geosci. Remote Sens.* 63, 1–17 (2025). https://doi.org/10.1109/TGRS.2025.3542614
19. He, R., Hu, B.-G., Zheng, W.-S., Kong, X.-W.: Robust principal component analysis based on maximum correntropy criterion. *IEEE Trans. Image Process.* 20(6), 1485–1494 (2011). https://doi.org/10.1109/TIP.2010.2103949
20. Cui, Y., et al.: Mapping land-cover dynamics in arid regions using spectral mixture analysis and representative training samples. *IEEE Trans. Geosci. Remote Sens.* 62, 1–13 (2024). https://doi.org/10.1109/TGRS.2024.3472080
21. Gao, J., Shi, J., Zhu, F.: Robust sparse unmixing via continuous mixed norm to address mixed noise. *IEEE Geosci. Remote Sens. Lett.* (2025). https://doi.org/10.1109/LGRS.2025.3548697
22. Rasti, B., Zouaoui, A., Mairal, J., Chanussot, J.: Image processing and machine learning for hyperspectral unmixing: an overview and the HySUPP Python package. *IEEE Trans. Geosci. Remote Sens.* 62, 1–31 (2024). https://doi.org/10.1109/TGRS.2024.3393570
23. Leng, W., Han, X., Deng, J., Zhang, H., Li, W., Sun, W.: Spectral super-resolution by using universal and private jointed spectral library and its applications. *IEEE Trans. Geosci. Remote Sens.* 62, 1–11 (2024). https://doi.org/10.1109/TGRS.2024.3405528
24. Ma, Y., Cai, S., Zhou, J.: Adaptive reference-related graph embedding for hyperspectral anomaly detection. *IEEE Trans. Geosci. Remote Sens.* 61, 1–14 (2023). https://doi.org/10.1109/TGRS.2023.3249344
25. Grupo de Inteligencia Computacional (GIC), Pavia University: Hyperspectral Remote Sensing Scenes. https://www.ehu.eus/ccwintco/index.php?title=Hyperspectral_Remote_Sensing_Scenes#Pavia_University_scene (accessed May 2025)
26. ECOSTRESS Spectral Library. https://speclib.jpl.nasa.gov (accessed May 2025)